Applied Radiation and Isotopes 194 (2023) 110708

Contents lists available at ScienceDirect

Applied Radiation and Isotopes

journal homepage: www.elsevier.com/locate/apradiso

Determination of the half-life of gadolinium-148

Nadine M. Chiera [a,*], Rugard Dressler [a], Peter Sprung [b], Zeynep Talip [a,c], Dorothea Schumann [a]

[a] Laboratory of Radiochemistry, Paul Scherrer Institut, Villigen, PSI, Switzerland
[b] Department Hot Laboratory, Paul Scherrer Institut, 5232, Villigen, PSI, Switzerland
[c] Center for Radiopharmaceutical Sciences ETH-PSI-USZ, Paul Scherrer Institut, Villigen, PSI, Switzerland

ARTICLE INFO

Keywords:
Gd-148
Half-life
ERAWAST
Exotic radionuclide
Radio-lanthanide

ABSTRACT

The half-life of the alpha-emitter ^{148}Gd was measured using the "direct method", in which the number of atoms is directly determined and their activity is then measured. Pure Gd samples containing megabecquerels of ^{148}Gd were obtained by reprocessing proton-irradiated tantalum material. Multicollector-inductively coupled plasma mass spectrometry was performed to determine the amount of ^{148}Gd atoms retrieved. The activity of the ^{148}Gd atoms contained in the Gd sample was measured by means of alpha-spectrometry. The half-life of ^{148}Gd was deduced to be 86.9 years, with a combined uncertainty of 4.5%.

1. Introduction

Accurate nuclear decay data for the pure α-emitter ^{148}Gd (α-branching ratio $I_\alpha = 100\%$ at energy $E_\alpha = 3182.8$ keV (Nica, 2014)) is needed in various research fields, ranging from astrophysics to nuclear energy and safety. The determination of the ^{144}Sm(α,γ)^{148}Gd reaction rate *via* the activation method (Somorjai et al., 1998; Scholz et al., 2020), the calculation of neutron capture cross sections of ^{148}Gd (Rios et al., 2006), the evaluation of the toxicity of irradiated spallation targets for disposal (Artisyuk et al., 2002a), as well as the dose assessment in humans after ingestion or inhalation of ^{148}Gd (Artisyuk et al., 2002b), are prominent examples of studies that require highly precise ^{148}Gd half-life ($t_{1/2}$) data. During the course of the past decades, different half-life values for ^{148}Gd were reported, as summarized in Table 1.

The $t_{1/2} = (74.6 \pm 3.0)$ y (Prestwood et al., 1981), adopted by the ENDF/B-VIII.0 (Brown et al., 2018) and JEFF-3.3 (Plompen et al., 2020) databases, was recently confirmed – within the indicated uncertainties – by the work of Fülöp et al. (2003). However, the latter was given as a preliminary result after a two-years-long decay measurement. The finalization of this decay measurement is still pending. Given the scattered half-life values of ^{148}Gd available in literature, a $t_{1/2} = (71.1 \pm 1.2)$ y was calculated in (Nica, 2014), as the weighted average of the results reported in (Prestwood et al., 1981) and (Fülöp et al., 2003). The derived value is currently adopted in nuclear databases such as the Karlsruhe Nuclide Chart (Sóti et al., 2019) and in the NUBASE2020 data collection (Kondev et al., 2021). However, as commented in (Plompen et al., 2020), a least squares weighted analysis of the half-life values given in (Siivola, 1962), (Friedman et al., 1966), and (Prestwood et al., 1981) points instead to a $t_{1/2} = (83.4 \pm 10.8)$ y. Although this calculation takes into consideration the majority of the ^{148}Gd half-life determinations performed up to now, the mentioned value is impractical for high-precision calculations since it is affected by a relative uncertainty of about 13%.

In this work, the half-life of ^{148}Gd was re-measured by applying the *direct method*. In the framework of the ERAWAST (Exotic Radionuclides from Accelerator Waste for Science and Technology) project (Schumann and Neuhausen, 2007; Schumann et al., 2013), sufficient amounts of radiochemically pure ^{148}Gd were obtained by reprocessing proton irradiated tantalum targets (Dai et al., 2005) already available at the Paul Scherrer Institute (PSI). Successively, the number N of ^{148}Gd atoms was determined using multicollector inductively-coupled plasma mass spectrometry (MC-ICP-MS), whereas their activity A was measured by means of α-spectroscopy. In order to obtain high-resolution α-spectra, thin and homogeneous radioactive sources were prepared with the molecular plating technique – also referred to as electrostatic deposition (Parker and Falk, 1962; Ko, 2020). Finally, by applying Equation (1), the half-life of ^{148}Gd was derived:

$$t_{1/2} = \ln(2)\frac{N}{A} \quad (1)$$

According to the *Guide to the expression of uncertainty in measurement – GUM* recommendations (ISO/IEC Guide 98-3, 2008; Bich et al., 2012), an uncertainty budget for the measured half-life is provided as well.

* Corresponding author.
E-mail address: nadine-mariel.chiera@psi.ch (N.M. Chiera).

https://doi.org/10.1016/j.apradiso.2023.110708
Received 19 December 2022; Accepted 27 January 2023
Available online 28 January 2023
0969-8043/© 2023 The Authors. Published by Elsevier Ltd. This is an open access article under the CC BY license (http://creativecommons.org/licenses/by/4.0/).

Table 1
Half-life ($t_{1/2}$) values for ^{148}Gd in literature.

Half-life (y)	Year	Detection method	Reference
~140	1953	Yield of ^{148}Gd estimated from ^{147}Sm(α,3n)^{148}Gd	J.O. Rasmussen (Rasmussen et al., 1953)
84 ± 9	1962	No information available	A. Siivola (Siivola, 1962)
97.5 ± 6.5	1966	Isotope dilution, mass spectrometry for number of atoms	A. M. Friedman (Friedman et al., 1966)
74.6 ± 3.0	1981	Isotope dilution, mass spectrometry for number of atoms	R. J. Prestwood (Prestwood et al., 1981)
70.9 ± 1.0	2003	Decay measurement, preliminary result	Zs. Fülöp (Fülöp et al., 2003)

2. Experimental

Separation: A pure Gd fraction containing ^{148}Gd was extracted from Ta samples irradiated with protons and spallation neutrons during the second SINQ Target Irradiation Program at PSI (Dai et al., 2005). The Gd was extracted from the radioactive Ta matrix with the methodology reported in (Talip et al., 2017), and separated from other lanthanides and spallation products by applying a series of ion-exchange chromatographic columns, as described in (Chiera et al., 2020). During separation, the short-lived γ-ray emitter ^{153}Gd ($t_{1/2}$ = 144.4 d, E_γ (29%) = 97.43 keV (Nica, 2020)) was added as an internal radiotracer. The separated Gd fraction in 1 M HNO_3 phase (here referred to as "Gd master solution") was then analyzed by mass-spectrometry without further purification.

Mass-spectrometry analysis: The absolute number of ^{148}Gd atoms in the retrieved fraction was determined by "reverse isotope dilution" (Vogl and Pritzkow, 2010) and "gravimetric standard addition with an additional internal standard" (Hauswaldt et al., 2012), with the internal standard being here ^{nat}Eu. In the latter method, the stable Gd nuclide ion beam intensities are normalized to the ion beam intensities of ^{151}Eu and ^{153}Eu, resulting in a technique equivalent to the gravimetric standard addition. However, the increase in the Eu-normalized ion beam intensity ratios (e.g., ^{152}Gd/^{151}Eu and ^{152}Gd/^{153}Eu) with increasing the amounts of gravimentrically added Gd standard, is given. This treatment eliminates variations in ionization efficiency and plasma fluctuations, allowing for more precise determinations of elemental mass fractions. All mass-spectrometric measurents were conducted on the Nu Instruments Plasma 3 MC-ICP-MS at the Hotlaboratory Department of PSI. Ions at masses 142, 145, 147–157, 159, 160, and 163 on Faraday cups connected to amplifier systems with a 10^{11} Ω resistor in their feedback loop were simultaneously collected. The analytes were introduced in 0.28 M HNO_3 using an Elemental Scientific APEX HF nebulizing system and a self-aspiring Elemental Scientific PFA-ST Microflow at a consumption rate of ca. 50 μl min^{-1}. The plasma was operated at 1350 W forward power. All analytes were repeatedly measured (17–21 repetitions per analyte) at 1) high mass resolution, 2) medium mass resolution, and 3) low mass resolution setting with at least 3 repetitions per resolution setting to assess possible effects from molecular interferences at lower mass resolution. Online instrumental mass discrimination was corrected applying the exponential mass discrimination law (Russell et al., 1978). A first online correction used ^{nat}Eu (He et al., 2020a). A subsequent offline reprocessing was implemented to improve the accuracy of the mass discrimination correction. For this, the online correction was mathematically adjusted on the basis of the observed relative magnitude of Gd and on the online acquired Eu-based mass discrimination information (Chang et al., 1994). The latter was defined by analyzing at matching intensities mixed Eu–Gd standard solutions alongside the samples during each measurement session. The same mixed Eu–Gd standard solutions, measured during each analytical session, further provided a common normalizing reference for all ^{xxx}Gd/^{yyy}Eu values used in standard addition calculations, where xxx stands for the nominal mass of the involved stable Gd nuclides (152, 154, 155–157) and yyy for ^{151}Eu and ^{153}Eu. This allowed for cancelling out daily variations in the relative sampling of Eu and Gd within the expanding plasma at the interface cones of the mass spectrometer.

A certified Mettler-Toledo XP56 balance (10^{-6} g scale interval) was used in all the gravimetric steps, in a room at a controlled temperature of 20–23 °C. Since the buoyancy difference between the calibration weights used during certification of the balance and the weighed solution is below 0.055%, systematic uncertainties regarding the weighting process were considered negligible.

Radioactive source preparation: The ^{148}Gd radioactive source was prepared using the molecular plating technique. An aliquot of (0.516547 ± 0.000040) g (see Table 2) of the Gd master solution was used.

In order to deduce the number of atoms of ^{148}Gd plated on the deposition foil (graphite foil, thickness: 75 μm, purity: 99.8%, Flexible Graphite, GoodFellow), the molecular plating yield was followed by measuring the ^{153}Gd γ-tracer contained in the Gd aliquote before deposition, and comparing it to the count rate of the ^{153}Gd deposited on the graphite foil. Since the chemical behavior of ^{148}Gd and ^{153}Gd is identical, the plating yield deduced for ^{153}Gd corresponds hence to the one for ^{148}Gd. Both γ-ray spectroscopy measurements before and after deposition were conducted with a BEGe™ (Broad Energy Germanium γ-ray detector, Mirion Technologies (Canberra), Inc.). Energy calibration was done with a^{152}Eu ($t_{1/2}$ = 13.53 y, I_γ = 28.41% at E_γ = 121.78 keV (Martin, 2013)) point-source from Physikalisch-Technische Bundesanstalt (PTB). The FWHM (Full Width at Half Maximum) was 0.616 keV at 97.4 keV. Data acquisition and analysis were done using the Genie™ 2000 Gamma Acquisition & Analysis Software.

For a reliable comparison of the activity of the ^{153}Gd contained in the Gd aliquot and the activity of the ^{153}Gd deposited in the thin Gd layer, both γ-ray measurements were performed in equal geometries by using the very same custom-made holder (see Fig. 1), following the method described in (Chiera et al., 2022). The γ-ray measurement of the ^{153}Gd contained in the aliquot before deposition (namely, "Measurement A") was performed for 28800 s. Successively, the plating solution was prepared. The Gd aliquot was dried at 70 °C under a N_2 flow, and then dissolved in 3 ml of 0.1 M HNO_3. The solution was again evaporated at 70 °C under a N_2 flow, re-dissolved in 10 ml of isopropanol (iPrOH), and put in an ultrasonic bath for 5 min at normal temperature and pressure conditions. The molecular plating cell used for the deposition of Gd on the graphite foil is described in (Maugeri et al., 2017). Before deposition, the plating cell, the graphite foil (75 μm), and the Pt wire (anode) were rinsed with iPrOH. The copper block (cathode), was cleaned with citric acid 0.1 M, and successively rinsed with MilliQ-2 water and iPrOH, in this very same order. To maintain a constant temperature of 15 °C during deposition, the cell was equipped with a Peltier cooler at the cathode. The prepared Gd solution in iPrOH was transferred to the

Table 2
Amount (in grams, g) of Gd aliquot of master solution, calculated as the difference between gross weight (vial with Gd aliquot) and tare (empty vial), used in the preparation of the Gd radioactive source with the molecular plating technique. The mean, the standard deviation (SD), and the uncertainty of ten consecutive weightings are indicated.

Weighting n°	Empty vial (g)	Vial with Gd aliquot (g)	Gd aliquot (g)
1	6.7648	7.28159	0.51679
2	6.76489	7.28167	0.51678
3	6.76496	7.28164	0.51668
4	6.7651	7.28167	0.51657
5	6.76508	7.28169	0.51661
6	6.76512	7.28164	0.51652
7	6.76517	7.28165	0.51648
8	6.76526	7.28167	0.51641
9	6.76533	7.28163	0.5163
10	6.76532	7.28165	0.51633
Mean	6.765103	7.28165	0.516547
SD	0.000178	0.000028	–
Uncertainty	0.000060	0.000012	0.000061

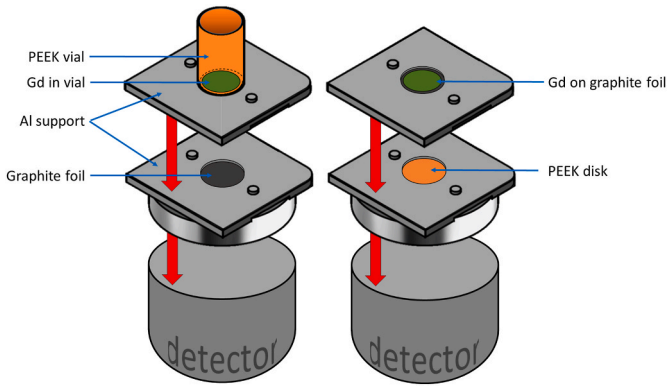

Fig. 1. Scheme of the custom-made sample holder for the measurement of the ^{153}Gd γ-ray tracer before molecular plating, and after deposition on the graphite foil for the deduction of the deposition yield. PEEK = Polyether ether ketone.

plating cell, and the deposition of Gd on the graphite foil was achieved in 4 h by applying a constant voltage of 100 V (starting current: 2.58 mA). During deposition, the distance between the two electrodes was 10 mm. After completion of the molecular plating, the γ-ray measurement of the ^{153}Gd deposited on the graphite foil (namely, "Measurement B") was performed for 1209600 s (i.e., 14 days).

α-measurement: The activity of the ^{148}Gd plated on the graphite foil was quantified by α-spectrometry using the Alpha Analyst Integrated Alpha Spectrometer (model A-450-21AM, Canberra) equipped with a silicon semiconductor detector (Passivated Implanted Planar Silicon – PIPS. Detector area: 450 mm^2). Data acquisition and analysis were done using the Genie™ 2000 Alpha Analysis Software. Energy calibration of the detector was performed with a mixed source of ^{239}Pu ($t_{1/2}$ = 2.41 y, I_α = 70.77% at E_α = 5.157 MeV (Browne and Tuli, 2014)), ^{241}Am ($t_{1/2}$ = 432.8 y, I_α = 84.8% at E_α = 5.486 MeV (Nesaraja, 2015)), and ^{244}Cm ($t_{1/2}$ = 18.1 y, I_α = 76.90% at E_α = 5.805 MeV (Akovali, 2003)) α-source. A FWHM of 34 keV was reached, with a sample-to-detector distance (SDD) of 10.4 mm. The efficiency of the α-counting was derived by measuring the count rate of a certified ^{241}Am source (PTB, calibration reference n° PTB-6.11-2016-1769) with activity A = (539.0 ± 5.5) Bq @01.11.2016 00:00:00 MEZ (uncertainty with k = 1), having the same diameter (20 mm) as the Gd deposition area on the graphite foil. Geometrical differences between the ^{241}Am standard source and the Gd plated sample were further minimized by using custom-made sample holders with identical SDDs. The α-spectrometry measurement of the deposited Gd layer was conducted for 500 s.

3. Results and discussion

Mass spectrometry analyses performed at 1) high mass resolution, 2) medium mass resolution, and 3) low mass resolution settings yielded consistent results. Interferences from Nd and Dy were monitored and found to be insignificant, i.e., ^{156}Dy/(^{156}Gd+^{156}Dy) < 2 × 10^{-5} and ^{148}Nd/(^{148}Gd+^{148}Nd) < 4.2 × 10^{-4}, assuming natural isotopic composition for these elements (Zhao et al., 2005; Chang et al., 2001; He et al., 2020b). Interferences from ^{148}Sm, monitored using ^{147}Sm, yielded ^{148}Sm/(^{148}Gd+^{148}Sm) < 1.9 × 10^{-2} assuming natural isotopic composition of Sm (Chang et al., 2002). This assumption is supported by the complete removal of Sm with the here applied separation procedure, as shown in (Chiera et al., 2020). Furthermore, the Sm level of impurity is identical in all solutions, including the mixed Gd–Eu standards. In particular, ^{147}Sm/^{151}Eu = 4.72 ±0.30 × 10^{-5} (1 s.d.) in the sample solutions and ^{147}Sm/^{151}Eu = 4.84 ±0.17 × 10^{-5} (1 s.d.) in the mixed Gd–Eu standards. Moreover, the ^{149}Sm/^{147}Sm values in the sample solutions and in the Gd–Eu standards differ by less than 1% (±4%, 1 s.d.) on average, with the values of Gd–Eu standards being bracketed by those of the sample solutions. Furthermore, the measured ^{148}Sm/^{150}Sm values of all sample solutions are identical within 1 s.d. of ≪ 0.05% independent of the amount of Gd standard added. It is thus conceivable that the same pool of Sm – likely from the Eu standard – dominates the Sm impurities in all solutions. Therfore the assumption of natural Sm isotopic abundaces for interference corrections from Sm is accurate. The number of ^{148}Gd atoms contained in the master solution was obtained by multiplying two instances defined by MC-ICP-MS measurements with the dilution factor to the master solution: 1) the obtained ^{148}Gd/$^{152,154\text{-}157}$Gd values of the pure Gd fraction and 2) the respective number of stable $^{152,154\text{-}157}$Gd atoms in the same solution. The number of stable $^{152,154\text{-}157}$Gd atoms was determined by both reverse isotope dilution (Vogl and Pritzkow, 2010) using ^{148}Gd as an isotope tracer, as well as by standard addition using an additional standard (Hauswaldt et al., 2012). The ^{148}Gd content determined by both methods is identical within 2 standard deviations. The concentration of ^{148}Gd in the retrieved fraction was quantified as (0.3820 ± 0.0038) nmols per gram of solution (solvent: 1 M HNO_3), with a combined uncertainty of 0.99% (k = 1). γ-ray spectroscopy measurements of the Gd solution before electrodeposition has shown the activity of ^{153}Gd being (0.4421 ± 0.0058) counts•s^{-1} @03.03.2021. After molecular plating, the activity of the ^{153}Gd tracer deposited on the foil was determined to be (0.0073 ± 0.0003) counts•s^{-1}. Details on the deduced count rates are given in Table 3. The γ-ray spectra of both ^{153}Gd measurements before and after deposition are shown in Fig. 2.

Considering the decay of the ^{153}Gd tracer between the two activity measurements (before deposition and the measurement after deposition, i.e., 210 days), a (3.18 ± 0.13)% plating yield was obtained. The uncertainty on the plating yield includes the 1.42% uncertainty on the geometry correction factor deduced in (Chiera et al., 2022) which allows a direct comparison of the count rate of the ^{153}Gd in solution and the count rate of the ^{153}Gd deposited on the graphite foil, as well as takes into account the 0.42% uncertainty on the half-life of the ^{153}Gd tracer (Nica, 2020). The amount of ^{148}Gd plated on the graphite foil corresponds hence to (3.778 ± 0.038) × 10^{12} atoms. From the α-spectrum (see Fig. 3) of ^{148}Gd deposited on the graphite foil, an activity of (955 ± 13) Bq was deduced. Details for the ^{148}Gd activity measurement are presented in Table 4.

By applying Equation (1), a half-life of (86.9 ± 3.9) y for ^{148}Gd was obtained. The uncertainty budget is presented in Table 5.

4. Conclusions

In this work, a half-life value of (86.9 ± 3.9) y for ^{148}Gd was determined, with a combined standard uncertainty of 4.5% (k = 1). This result is in agreement with the $t_{1/2}$ = (84 ± 9) y value from (Siivola, 1962), and it is as well in agreement, within the error bars, with the (97.5 ± 6.5) y half-life value reported in (Friedman et al., 1966). The result obtained in this work is also in line with the weighted average of the half-life values given in (Siivola, 1962), (Friedman et al., 1966), and (Prestwood et al., 1981), i.e., $t_{1/2}$ = (83.4 ± 10.8) y. It is recommended therefore to adopt the result presented in this work for calculations that use the ^{148}Gd half-life as a parameter.

Table 3
Count rate (in counts•s^{-1}) at 97.4 keV corresponding to the γ-ray measurements of ^{153}Gd contained in the Gd aliquot before molecular plating (Measurement A) and in the deposited Gd layer (Measurement B). The exact dates (in dd.mm.yyyy format) at which the measurements were performed are given. The real time (t_{real}, in s) and life time (t_{life}, in s) of each measurement are reported as well.

	Date (dd.mm.yyyy)	t_{real} (s)	t_{life} (s)	Count rate (counts•s^{-1})
Measurement A	03.03.2021	28800	28800	0.4421 ± 0.0058
Measurement B	29.09.2021	1209600	1209143	0.0073 ± 0.0003

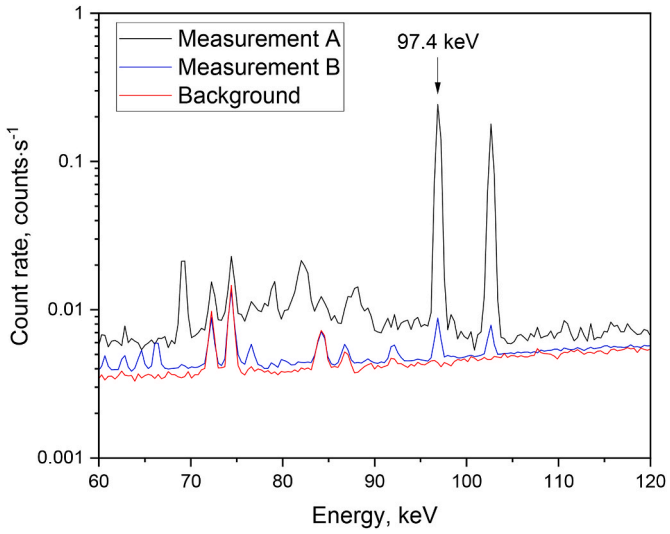

Fig. 2. Count rate (in counts•s^{-1}) of the ^{153}Gd contained in the Gd aliquot before molecular plating (Measurement A, black line) and of the ^{153}Gd deposited on the graphite foil (Measurement B, blue line). The background is reported as well (red line). The reference peak for ^{153}Gd is indicated.

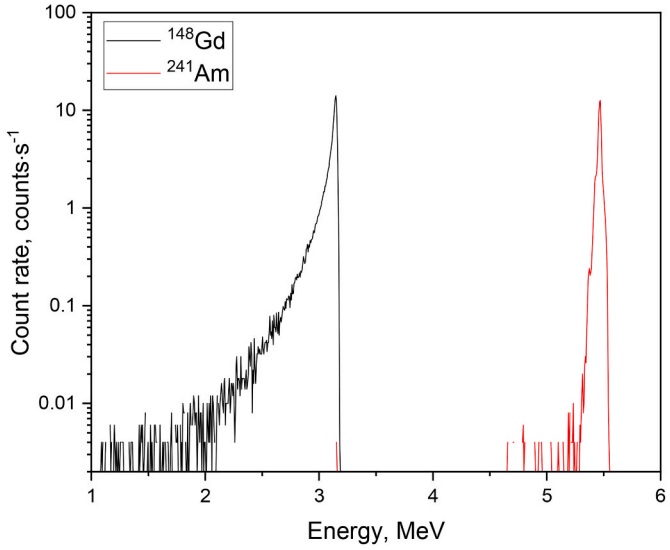

Fig. 3. Count rate (in counts•s^{-1}) of the deposited ^{148}Gd on the graphite foil (black line) and the standard calibration source ^{241}Am (red line).

Table 4
Activity (in Bq) of the ^{148}Gd deposited on the graphite foil. The activity of the ^{241}Am standard source used for efficiency calibration is indicated as well. For each measurement, the real time (t_{real}, in seconds) and the life time (t_{life}, in seconds) is given. The energy range considered for the calculation of the count rate (in counts•s^{-1}) of each α-peak is specified.

	t_{real} (s)	t_{life} (s)	Energy range (MeV)	Count rate (counts•s^{-1})	Activity (Bq)
^{241}Am	500	501	5.3–5.6	78.84 ± 0.56	534.9 ± 5.5 [a]
^{148}Gd	500	500	1.0–3.2	140.82 ± 0.75	955 ± 13

[a] Activity of the source at the date of the efficiency calibration (20.07.2021), calculated using (432.6 ± 0.6) y as the half-life of ^{241}Am, as reported in (Nesaraja, 2015).

Table 5
Uncertainty budget (with k = 1) for the measured ^{148}Gd half-life.

Parameter	Uncertainty	Partial contribution	
^{148}Gd in master solution	0.99%		
Weighting	0.055%		
Deposition yield	4.13%		
		^{153}Gd γ-activity before plating	1.31%
		^{153}Gd γ-activity after plating	3.63%
		Correction factor	1.42%
		Gd aliquot mass	0.012%
		$t_{1/2}$ ^{153}Gd	0.42%
^{153}Gd activity	1.36%		
		^{148}Gd α-activity	0.53%
		^{241}Am α-activity	0.71%
		^{241}Am ref. standard	1.02%
		$t_{1/2}$ ^{241}Am	0.14%
Total	**4.5%**		

CRediT authorship contribution statement

Nadine M. Chiera: Conceptualization, Data curation, Formal analysis, Investigation, Methodology, Project administration, Visualization, Writing – original draft, Writing – review & editing. **Rugard Dressler:** Conceptualization, Data curation, Formal analysis, Validation, Writing – review & editing. **Peter Sprung:** Data curation, Formal analysis, Investigation, Writing – review & editing. **Zeynep Talip:** Conceptualization, Writing – review & editing. **Dorothea Schumann:** Conceptualization, Funding acquisition, Project administration, Resources, Supervision, Validation, Visualization, Writing – review & editing.

Declaration of competing interest

The authors declare the following financial interests/personal relationships which may be considered as potential competing interests: Dorothea Schumann reports financial support was provided by Swiss National Science Foundation.

Data availability

Data will be made available on request.

Acknowledgments

This project is funded by the Swiss National Science Foundation (SNF grant no 200021-159738).

References

Akovali, Y.A., 2003. Nuclear data sheets for A= 244. Nucl. Data Sheets 99 (1), 197–273.
Artisyuk, V., Saito, M., Stankovskii, A., Yu, Korovin, Shmelev, A., 2002a. Radiological hazard of long-lived spallation products in accelerator-driven system. Prog. Nucl. Energy 40 (3–4), 637–645.
Artisyuk, V., Saito, M., Stankovskii, A., Yu, Korovin, Shmelev, A., 2002b. Radiological hazard of long-lived spallation products in accelerator-driven system. Prog. Nucl. Energy 40 (3–4), 637–645.
Bich, W., Cox, M.G., Dybkaer, R., Elster, C., Estler, W.T., Hibbert, B., Imai, H., et al., 2012. Revision of the 'Guide to the expression of uncertainty in measurement. Metrologia 49 (6), 702.
Brown, D.A., Chadwick, M.B., Capote, R., Kahler, A.C., Trkov, A., Herman, M.W., Sonzogni, A.A., et al., 2018. ENDF/B-VIII. 0: the 8th major release of the nuclear reaction data library with CIELO-project cross sections, new standards and thermal scattering data. Nucl. Data Sheets 148, 1–142.
Browne, E., Tuli, J.K., 2014. Nuclear data sheets for A= 239. Nucl. Data Sheets 122 (no. 1), 293–376.
Chang, T.L., Qian, Q.Y., Zhao, M.T., Wang, J., 1994. The absolute isotopic composition of europium. Int. J. Mass Spectrom. Ion Process. 139, 95–102.
Chang, T.-L., Li, W.-J., Zhao, M.-T., Wang, J., Qian, Q.-Y., 2001. Absolute isotopic composition and atomic weight of dysprosium. Int. J. Mass Spectrom. 207 (1–2), 13–17.
Chang, T.-L., Zhao, M.-T., Li, W.-J., Wang, J., Qian, Q.-Y., 2002. Absolute isotopic composition and atomic weight of samarium. Int. J. Mass Spectrom. 218 (2), 167–172.

Chiera, N.M., Talip, Z., Fankhauser, A., Schumann, D., 2020. Separation and recovery of exotic radiolanthanides from irradiated tantalum targets for half-life measurements. PLoS One 15 (7), e0235711.
Chiera, N.M., Dressler, R., Sprung, P., Talip, Z., Schumann, D., 2022. High precision half-life measurement of the extinct radio-lanthanide dysprosium-154. Sci. Rep. 12 (1), 1–10.
Dai, Y., Jia, X., Thermer, R., Hamaguchi, D., Geissmann, K., Lehmann, E., Linder, H.P., et al., 2005. The second SINQ target irradiation program, STIP-II. J. Nucl. Mater. 343 (1–3), 33–44.
Friedman, A.M., Milsted, J., Metta, D., Henderson, D., Lerner, J., Harkness, A.L., Rok Op, D.J., 1966. Alpha decay half lives of ^{148}Gd, ^{150}Gd, and ^{146}Sm. Radiochim. Acta 5 (4), 192–194.
Fülöp, Z., Bartha, L., Gyurky, G., Somorjai, E., Kubono, S., Kudo, H., Kaji, D., 2003. The half-life of Gd-148. Nucl. Phys. 718, 688C–690C.
Hauswaldt, A.L., Rienitz, O., Jährling, R., Fischer, N., Schiel, D., Labarraque, G., Magnusson, B., 2012. Uncertainty of standard addition experiments: a novel approach to include the uncertainty associated with the standard in the model equation. Accred Qual. Assur. 17 (2), 129–138.
He, J., Yang, L., Hou, X., Mester, Z., Meija, J., 2020a. Determination of the isotopic composition of gadolinium using multicollector inductively coupled plasma mass spectrometry. Anal. Chem. 92 (8), 6103–6110.
He, J., Yang, L., Hou, X., Mester, Z., Meija, J., 2020b. Determination of the isotopic composition of gadolinium using multicollector inductively coupled plasma mass spectrometry. Anal. Chem. 92 (8), 6103–6110.
ISO/IEC Guide 98-3, 2008. Uncertainty of Measurement - Part 3: Guide to the Expression of Uncertainty in Measurement (GUM:1995). https://www.iso.org/standard/50461.html (2008).
Ko, Y.G., 2020. Preparation and characterization of electrodeposited layers as alpha sources for alpha-particle spectrometry. J. Radioanal. Nucl. Chem. 326 (2), 861–877.
Kondev, F.G., Wang, M., Huang, W.J., Naimi, S., Audi, G., 2021. The NUBASE2020 evaluation of nuclear physics properties. Chin. Phys. C 45 (3), 030001.
Martin, M.J., 2013. Nuclear data sheets for A= 152. Nucl. Data Sheets 114 (11), 1497–1847.
Maugeri, E.A., Heinitz, S., Dressler, R., Barbagallo, M., Kivel, N., Schumann, D., Ayranov, M., et al., 2017. Preparation of ^{7}Be targets for nuclear astrophysics research. J. Instrum. 12 (2), P02016.
Nesaraja, C.D., 2015. Nuclear data sheets for A= 241. Nucl. Data Sheets 130 (1), 183–252.
Nica, N., 2014. Nuclear data sheets for A= 148. Nucl. Data Sheets 117, 1–229.
Nica, N., 2020. Nuclear data sheets for A= 153. Nucl. Data Sheets 170, 1–498.
Parker, W., Falk, R., 1962. Molecular plating: a method for the electrolytic formation of thin inorganic films. Nucl. Instrum. Methods 16, 355–357.
Plompen, Arjan JM., Cabellos, O., De Saint Jean, C., Fleming, M., Algora, A., Angelone, M., Archier, P., et al., 2020. The joint evaluated fission and fusion nuclear data library, JEFF-3.3. The Eur. Phys. J. A 56 (7), 1–108.
Prestwood, R.J., Curtis, D.B., Cappis, J.H., 1981. Half-life of Gd-148. Phys. Rev. C 24 (3), 1346.
Rasmussen Jr., J.O., Thompson, S.G., Ghiorso, A., 1953. Alpha-radioactivity in the 82-neutron region. Phys. Rev. 89 (1), 33.
Rios, M.G., Casperson, R.J., Krane, K.S., Norman, E.B., 2006. Neutron capture cross sections of Gd-148 and the decay of Gd-149. Phys. Rev. C 74 (4), 044302.
Russell, W.A., Papanastassiou, D.A., Tombrello, T.A., 1978. Ca isotope fractionation on the Earth and other solar system materials. Geochem. Cosmochim. Acta 42 (8), 1075–1090.
Scholz, P., Wilsenach, H., Becker, H.W., Blazhev, A., Heim, F., Foteinou, V., Giesen, U., et al., 2020. New measurement of the ^{144}Sm $(\alpha,\gamma)^{148}$Gd reaction rate for the γ process. Phys. Rev. C 102 (4), 045811.
Schumann, D., Neuhausen, J., 2007. Accelerator waste as a source for exotic radionuclides. J. Phys. G Nucl. Part. Phys. 35 (1), 014046.
Schumann, D., Stowasser, T., Dressler, R., Ayranov, M., 2013. Possibilities of preparation of exotic radionuclide samples at PSI for scientific investigations. Radiochim. Acta 101 (8), 501–508.
Siivola, A., 1962. On the alpha activity of neutron deficient europium and gadolinium isotopes. Ann. Acad. Sci. Fennicae, Ser. A. no 6.
Somorjai, E., Fülöp, Z., Kiss, A.Z., Rolfs, C.E., Trautvetter, H.P., Greife, U., Junker, M., Goriely, S., Arnould, M., Rayet, M., Rauscher, T., 1998. Experimental cross section of ^{144}Sm $(\alpha,\gamma)^{148}$Gd and implications for the p-process. Astron. Astrophys. 333, 1112–1116.
Sóti, Z., Magill, J., Dreher, R., 2019. Karlsruhe nuclide chart–new 10th edition 2018. EPJ Nuclear Sciences & Technologies 5, 6.
Talip, Z., Dressler, R., David, J.C., Vockenhuber, C., Muller-Gubler, E., Vogele, A., Strub, E., Vontobel, P., Schumann, D., 2017. Radiochemical determination of long-lived radionuclides in proton-irradiated heavy-metal targets: Part I-tantalum. Anal. Chem. 89 (24), 13541–13549.
Vogl, J., Pritzkow, W., 2010. Isotope dilution mass spectrometry - a primary method of measurement and its role for RM certification. MAPAN-J. Metrol. Soc. India 25 (3), 135–164.
Zhao, M., Zhou, T., Wang, J., Lu, H., Xiang, F., 2005. Absolute measurements of neodymium isotopic abundances and atomic weight by MC-ICPMS. Int. J. Mass Spectrom. 245 (1–3), 36–40.